

## NUMERICAL SIMULATION OF THE FLOW AROUND A SQUARE CYLINDER AT LOW REYNOLDS NUMBER: THE DOMAIN SIZE INFLUENCE

**Odenir de Almeida – odenir@dem.feis.unesp.br**

**Sérgio Said Mansur – mansur@dem.feis.unesp.br**

UNESP – Faculdade de Engenharia de Ilha Solteira, Departamento de Engenharia Mecânica  
15385-000 - Ilha Solteira, SP, Brasil

**Aristeu da Silveira Neto – aristeus@mecanica.ufu.br**

UFU – Faculdade de Engenharia Mecânica, Departamento de Engenharia Mecânica  
38400-902 - Uberlândia, MG, Brasil

**Abstract.** *The flow around a square cylinder at low Reynolds numbers has been simulated with different configurations, in order to study the effects of domain size on the fluid motion. Numeric two-dimensional calculations have been performed with FLUENT®5.0 software by means of a finite-volume method employing a structured grid. An incompressible SIMPLEC algorithm has been employed for the velocity-pressure coupling, and the third-order QUICK scheme has been used for the treatment of convective terms. The influence of blockage ratio, as well as inlet and outlet location on the flow, has been investigated. Numerical flow patterns are also presented by means of streamlines and vorticity contours for the blockage ratios studied. Quantitative parameters as Strouhal number, lift, drag and pressure coefficients have been calculated for each case, showing that the values obtained depend strongly of the domain size.*

**Keywords:** *Numerical simulation, finite-volume method, calculation domain, square cylinder, vortex street.*

### 1. INTRODUCTION

The intense research activity on flow around bluff bodies has contributed substantially to the understanding of various flow field related phenomena. Particularly, a great number of works using different methods of analysis have had the objective of investigating the alternate vortex shedding and its influence in the various practical applications.

In terms of experimental research, the hot wire anemometer and the laser Doppler Velocimeter are exhaustively used for the measurement of velocity or vortex frequency in the wake of cylindrical bodies. Recently, new techniques using, for example, fluorescence induced by laser and PIV, have been used for visualization of the flow patterns around such geometries. Concerning the use of numeric tools, the enormous increase on the processing of modern computers has made it possible to identify and to study several mechanisms responsible for instabilities at the cylinder's wake.

Since the pioneering numerical work by Fromm & Harlow (1963) many other researchers around the world have studied the flow around bodies of circular or square transversal section, allowing the observation of refined details of the flow.

In spite of the unquestionable validity of the CFD codes used, some care should be taken to calculate reliable numerical results. A common problem in the numerical solution of flows is the presence of false diffusion, due to the use of low order schemes in the numeric representation of convective terms in the Navier-Stokes equations. Besides, sometimes the use of inadequate or coarse meshes contributes to calculate results physically inconsistent. The numerical model employed to discretize the governing equations as well as the shape and dimension of the calculation domain also have a great influence on the results obtained. Particularly, in the case of square or rectangular cylinders, the presence of sharp corners hinders the numeric prediction of the flow field, due to the presence of strong velocity gradients in these regions.

In the literature, some authors present preliminary studies about the domain size and mesh refinement on the numerical calculation of vortex shedding of the flow around cylinders. Davis & Moore (1982) presented a numerical and experimental analysis of Strouhal number for rectangular cylinders, in the laminar state, with different grid refinement. Yu & Kareem (1997) investigated the influence of grid size, convective transport schemes and time-step size on computation of turbulent flow around a rectangular prism. A study on the domain size influence has also been done by Sohankar & Norberg (1995) that investigated the flow around a two-dimensional square cylinder at low Reynolds numbers. Particularly, in the last work, the results have shown a great influence of the domain size on the calculation of mean parameters of the flow.

The main purpose of the present work is to develop further studies on the influence of domain size on parameters computation of the flow around a square cylinder.

As a start, the principal governing parameter of this flow is defined as the Reynolds number:

$$Re = \frac{U_{\infty} B}{\nu} \quad (1)$$

The quantitative parameters investigated are the Strouhal number, mean and rms drag coefficient, rms lift coefficient, and base and stagnation pressure coefficients at centerline of cylinder. These parameter are defined respectively below:

$$St = \frac{fB}{U_{\infty}} \quad (2)$$

$$C_D = \frac{F_D}{\frac{1}{2} \rho U_{\infty}^2 A} \quad (3)$$

$$C_L = \frac{F_L}{\frac{1}{2} \rho U_{\infty}^2 A} \quad (4)$$

$$C_p = \frac{p - p_{ref}}{\frac{1}{2} \rho U_{\infty}^2} \quad (5)$$

where  $f$  is the fundamental frequency of vortex shedding,  $B$  is the characteristic length of the cylinder,  $U_\infty$  is the normal free stream velocity,  $\rho$  is the fluid density,  $\nu$  is the kinematic viscosity,  $F_D$  and  $F_L$  are the drag and lift forces acting over the cylinder,  $A$  is the frontal or projected area, and the numerator  $(p - p_{ref})$  represents the difference between the calculated pressure and an arbitrary reference pressure.

In this work, the calculations have been done for Reynolds number equal to 100, modifying the upstream and downstream size domain, as well as the blockage ratio, as described in the next section. The numerical calculations have been performed using FLUENT®5.0, with the SIMPLEC finite volume algorithm and the QUICK scheme for the convective transport terms.

## 2. NUMERICAL PROCEDURE

In this work the flow was assumed to be unsteady and two-dimensional with constant fluid properties. The computational grid is formed by a rectangular domain, structured on the Cartesian coordinate system with uniformly distributed meshes ( $\Delta x = \Delta y$ ) in both directions. The numerical simulations have been accomplished by the numerical code FLUENT®5.0, without any turbulence model, employing an incompressible SIMPLEC finite-volume algorithm (Patankar & Spalding, 1972). The space derivative terms have been discretized by the QUICK scheme (Leonard, 1979) for the convective terms, and by second-order central differences scheme for diffusive terms.

A marching time step of  $\Delta t' = 0,02$  was used employing a fully implicit scheme for the unsteady terms. A non-dimensional time was defined by the follow expression:

$$\tau = t' \cdot U_\infty / B \quad (6)$$

where  $t'$  is the computational time. The solution has advanced until the fully developed vortex street has been obtained characterized for a periodic variation in the mean variables of the flow field.

Figure 1 depicts the computational domain, where  $X_u$  and  $X_d$  are the upstream and downstream flow sections lengths, respectively, and  $H$  is the section height. The streamwise length of the square cylinder is defined as  $B$  and the dimensionless parameters as Strouhal and Reynolds number are defined with respect to this characteristic length.

The boundary conditions have been set as follows. At the upstream boundary, the inlet flow has been assumed to be uniform. At the outlet, a zero gradient boundary condition for  $U$  and the prescribed velocity zero for  $V$  has been used. A no-slip condition has been prescribed at the body surfaces ( $U = V = 0$ ). At the upper and lower boundaries the symmetry conditions have been used, simulating a frictionless wall ( $V = \partial U / \partial y = 0$ ).

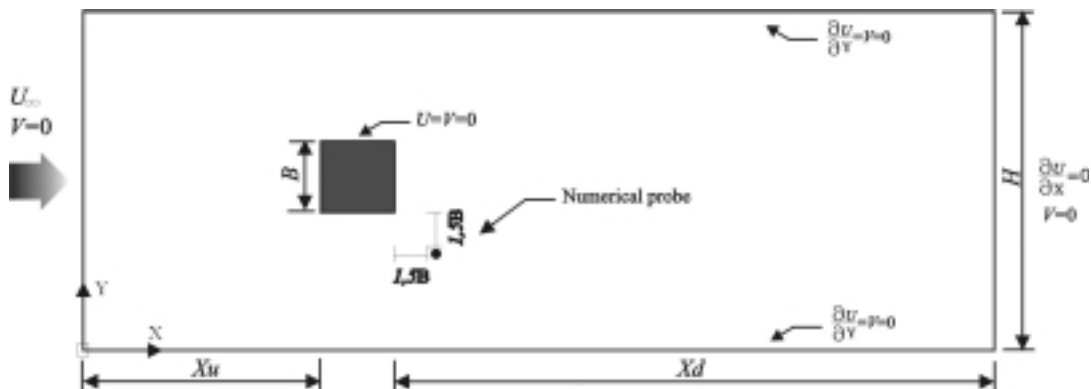


Figure 1 – Computational grid and boundary conditions.

Table 1 presents the different configurations of the domain for the cases investigated in this study. All numerical simulations, were conducted for  $Re = 100$ . The computational parameters registered are respectively Strouhal number ( $St$ ), mean drag coefficient ( $C_D$ ), rms drag coefficient ( $C_{D'}$ ), rms lift coefficient ( $C_L'$ ), stagnation pressure coefficient at centerline ( $C_{ps}$ ) and base pressure coefficient at centerline ( $C_{pb}$ ).

Table 1 – Outline of different configurations for the computational domain.

Case	Mesh	$Xu$	$Xd$	$H$
1	$226 \times 106$	$7B$	$20B$	$13B$
2	$250 \times 106$	$10B$	$20B$	$13B$
3	$282 \times 106$	$14B$	$20B$	$13B$
4	$170 \times 106$	$10B$	$10B$	$13B$
5	$202 \times 106$	$10B$	$14B$	$13B$
6	$250 \times 106$	$10B$	$20B$	$13B$
7	$330 \times 106$	$10B$	$30B$	$13B$
8	$490 \times 106$	$10B$	$50B$	$13B$
9	$250 \times 42$	$10B$	$20B$	$5B$
10	$250 \times 58$	$10B$	$20B$	$7B$
11	$250 \times 90$	$10B$	$20B$	$11B$
12	$250 \times 106$	$10B$	$20B$	$13B$
13	$250 \times 122$	$10B$	$20B$	$15B$
14	$250 \times 170$	$10B$	$20B$	$21B$

For the calculation of Strouhal number, a numerical probe was placed in the wake of the cylinder at a position of  $1,5B$  in the horizontal and vertical directions behind the obstacle. The temporal evolution of the  $y$ -component velocity was registered in the fully periodic regime of vortex formation and the numerical signal was processed by means of the Fast Fourier Transform (FFT), resulting in the fundamental frequency of vortex shedding.

### 3. RESULTS AND DISCUSSIONS

#### 3.1 Influence of Upstream Length

The influence of the upstream section length  $Xu$  was analyzed considering three different configurations. For the cases investigated, the value of downstream length was fixed at  $Xd = 20B$  and the height at  $H = 13B$ .

Table 2 presents the numerical values obtained for the different simulations. These results indicate that with the increase of upstream length  $Xu$ , there is a decrease in the values of the calculated parameters. Some differences are verified in the values of  $C_{pb}$  for cases (1) and (3).

According with the results, with increases of  $Xu$  from  $7B$  to  $14B$ , the values of mean drag coefficient decrease by approximately 2%, while the rms lift decrease by 3%. It is observed that there are not changes in the values of Strouhal number associated with the change in the upstream length.

The present analysis indicates that a good choice for the upstream region length is to work with values between  $10B < Xu < 14B$ . In the Table 2, values inferior to  $10B$  cause a notable influence over the parameters. On other hand, values superior to  $14B$  increase the processing time (CPU).

Table 2 – Influence of Upstream Length.

Case	$St$	$C_D$	$C_{D'}$	$C_{L'}$	$C_{ps}$	$-C_{pb}$
(1) – $Xu=7B$	0.144	1.6667	0.0038	0.1874	1.04	0.768
(2) – $Xu=10B$	0.144	1.6448	0.0037	0.1870	1.0	0.782
(3) – $Xu=14B$	0.144	1.6381	0.0037	0.1819	1.0	0.788

### 3.2 Influence of Downstream Length

The influence of downstream length was studied fixing the value  $Xu = 10B$  and the domain height  $H = 13B$ . The length  $Xd$  was varied in the range  $10B$  to  $50B$ . In this study the length of downstream domain has revealed a much greater relevance due to the association with the boundary condition employed in the outlet, zero gradient – Neumann type. It is well known that the use of this condition requires relatively larger values of  $Xd$  length, in order to have the unphysical disturbances associated with this boundary condition damped out.

The results obtained are presented in the Table 3. These results indicate that with an increase of downstream length, there is a decrease of some parameters as mean and rms drag coefficients, while the parameters as rms lift coefficient are increased. It should be observed that a further increase to  $Xd = 50B$  almost did not affect the parameters. An interesting fact verified in this work is related to the values obtained for the rms lift coefficient in cases (6), (7) and (8) that were about 40% higher than values obtained in the study of Sohankar & Norberg (1995). It should be also observed that the values for cases (4) and (5) were about 30% lower than the last value for case (8).

The major discrepancy verified in these values may be attributed to unphysical disturbances on the upstream flow created by the use of zero gradient as boundary condition at outlet. Therefore, the use of domains with downstream length above  $30B$  can be a good recommendation to simulations of this type. An alternative solution for this problem is the use of a convective boundary condition, described in the works of Sohankar *et al.* (1998) and Yu & Kareem (1997) that has presented good results in simulations of finite domain.

Table 3 – Influence of Downstream Length.

Case	$St$	$C_D$	$C_{D'}$	$C_{L'}$	$C_{ps}$	$-C_{pb}$
(4) – $Xd=10B$	0.144	1.6449	0.0040	0.1064	1.0	0.781
(5) – $Xd=14B$	0.144	1.6450	0.0038	0.1170	1.01	0.783
(6) – $Xd=20B$	0.144	1.6448	0.0037	0.1870	1.0	0.782
(7) – $Xd=30B$	0.144	1.6447	0.0038	0.1859	1.0	0.783
(8) – $Xd=50B$	0.144	1.6447	0.0038	0.1856	1.0	0.794

Again, it is verified that the downstream domain length does not affect the Strouhal number. Considering the great influence of  $Xd$  length on others parameters, the Strouhal number, in this case, is not the best indicator of variations in flow field. This observation was also registered by Sohankar *et al.* (1997).

According to results obtained, a good overall indicator of the variations and disturbances presents in the vortex shedding numerical calculation is the RMS lift coefficient. In fact, in the Table 3, it is verified that this parameter is quite sensitive to variations in the numerical flow field. Thus, a good recommendation for the computational domain, in this case, is to maintain  $Xd$  in the range  $20B$  to  $30B$ , since for values of  $Xd$  larger than  $30B$  the processing time is considerably increased.

### 3.3 Influence of Blockage

In the present study the influence of blockage ratio ( $\beta\%$ ) was investigated maintaining  $Xu = 10B$  and  $Xd = 20B$  constant. In this case, the blockage is not solid, since that the upper and lower boundaries of the domain were treated as frictionless walls, employing the symmetry boundary conditions ( $V = \partial U / \partial y = 0$ ).

Table 4 shows the results for the cases studied. It is observed that the Strouhal number was more sensitive to changes in the blockage ratio than in the previous cases investigated.

Table 4 – Influence of Blockage Ratio.

Case	$\beta\%$	$St$	$C_D$	$C_{D'}$	$C_{L'}$	$C_{ps}$	$-C_{pb}$
(9) – $H/B=5$	20	0.180	2.1966	0.0046	0.2519	1.0	1.380
(10) – $H/B=7$	14.28	0.162	1.8822	0.0038	0.1980	1.0	1.050
(11) – $H/B=11$	9.09	0.144	1.6828	0.0037	0.1865	1.0	0.830
(12) – $H/B=13$	7.69	0.144	1.6448	0.0037	0.1870	1.0	0.782
(13) – $H/B=15$	6.66	0.144	1.6210	0.0038	0.1846	1.0	0.763
(14) – $H/B=21$	4.76	0.126	1.5918	0.0040	0.1871	1.03	0.700

In this study, as blockage ratio increases also does the Strouhal number. In fact, an increase of 40% in the blockage amounts to an increase of about 11% in the Strouhal number.

A comparison between the cases studied reveals that at high blockage ratio the flow parameters assume bigger values, particularly for the base pressure coefficient. It will be seen later that changes in the blockage ratio affect the flow pattern considerably.

According to Sohankar (1995) one characteristic of the blockage effect is an effective increase in the oncoming velocity of the flow. In fact, since the cylinder area subject to perpendicular flow increases, the flow velocity around the cylinder tends to rise as well.

The present study indicates that, to keep the flow disturbances low, a suitable recommendation for the domain height may to be situated between  $15B$  and  $17B$ , that corresponds to blockage ratios of  $\beta = 6,66\%$  and  $\beta = 5,8\%$  respectively.

Finally, it is important to emphasize that in the Sohankar's (1998) work the use of QUICK scheme for a blockage less than 3% exhibited unphysical oscillations in the calculations. Further investigations show that unphysical oscillations are caused by too coarse a grid in the far field of the computational domain. In this case, the unbounded QUICK scheme is more sensitive to coarser grids than, for example, a two-order convective scheme.

#### *Streamlines and Vorticity contours at various blockage ratios*

The blockage ratio effect on the flow field around a square cylinder is shown on Figures (2), (3) and (4), through the streamlines and vorticity contours. As it can be seen from these figures, at high blockage the von Kármán street vortices are less stretched and more densely formed causing a strong curvature in the streamlines.

It is interesting to observe that for  $\beta = 4,76\%$ , the value of Strouhal number obtained is smaller than experimental data – in Okajima (1982). This discrepancy can be associated with numerical oscillations when using the QUICK scheme for minors blockage ratios, as pointed by Sohankar (1998). This oscillation in the flow field can be controlled using sub-grid scale modeling for turbulence, which will be studied in the sequence of this work.

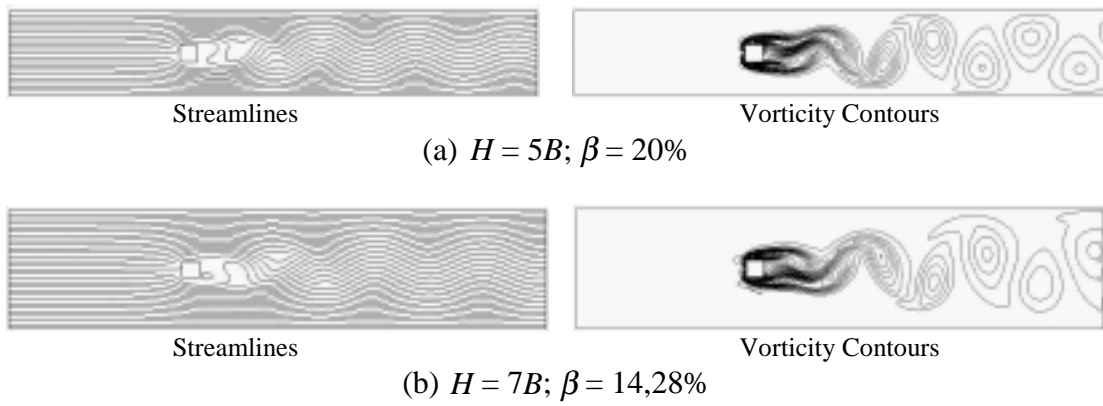


Figure 2 – Instantaneous streamlines and vorticity contours for different blockage ratios.

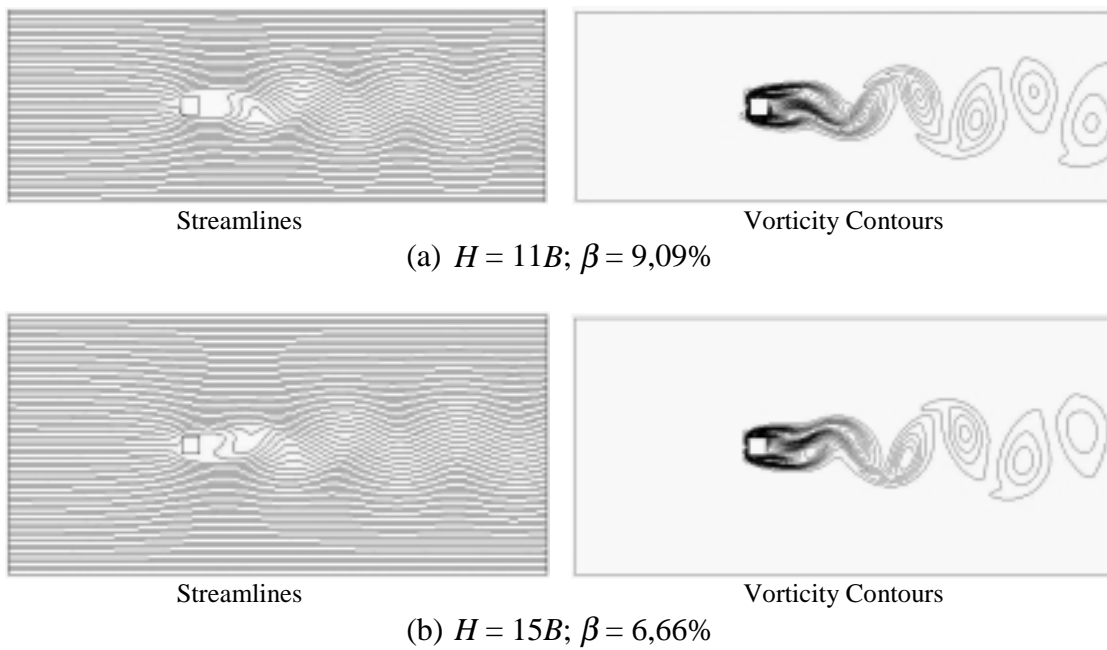


Figure 3 – Instantaneous streamlines and vorticity contours for different blockage ratios.

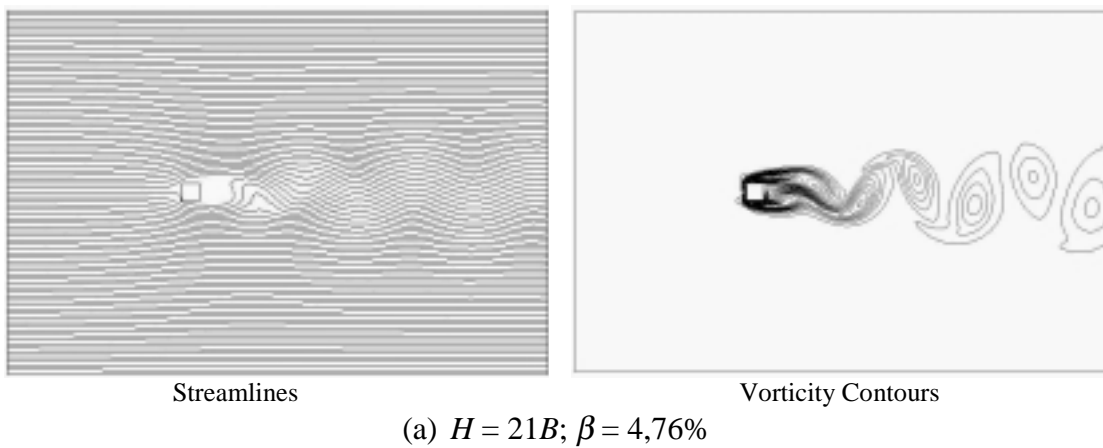


Figure 4 – Instantaneous streamlines and vorticity contours at different blockage ratios.

### 3.4 Extension of Results

For to validate the recommended values for the size domain investigated in this work, additional simulations has been conducted for Reynolds numbers ranged of  $10^2$  to  $10^3$ . The Figure 5 presents the curve Strouhal vs Reynolds for Reynolds number below  $10^3$ . For this calculation, it was used one of the recommended computational domains, fixing the characteristics dimensions in  $Xu = 10B$ ,  $Xd = 20B$  and  $H = 15B$ .

This domain was chosen based on the results obtained in the previous sections, which lead to the best values for the representative parameters of the flow field. The results used for comparison with the numerical results are data obtained experimentally in a water tunnel. For more details, see the indicated reference – Lindquist (2000).

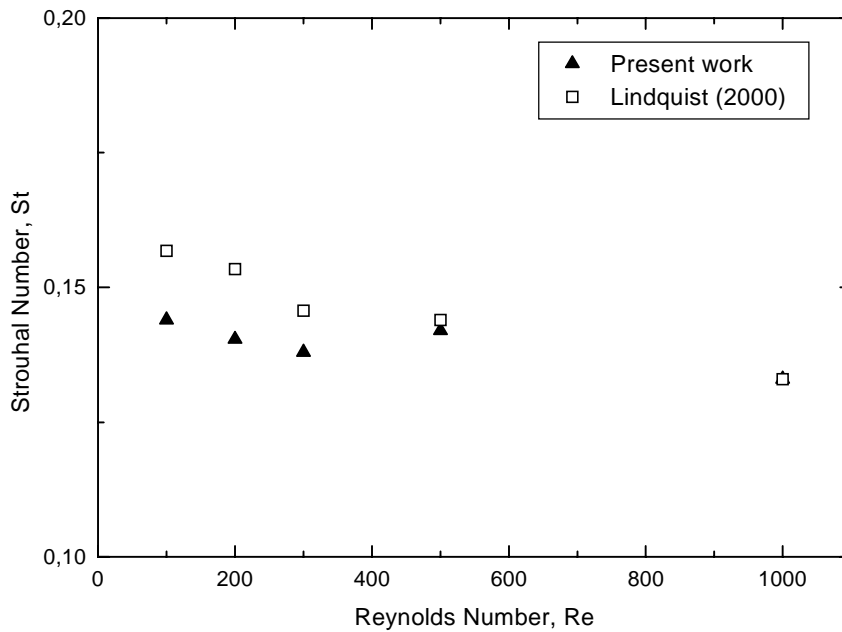


Figure 5 – Strouhal vs Reynolds curve.

Although the domain size influence was investigated for the Reynolds number 100 so far, the utilization of the chosen grid provides a good agreement between the numerical and experimental calculation of the Strouhal number along the range of Reynolds number calculated.

### 4. CONCLUDING REMARKS

The study of the influence of domain size on computation of unsteady flow around a square cylinder has been conducted for low-Reynolds number ( $Re = 100$ ). The influence of each parameter has been studied separately, as upstream and downstream lengths and height of computational domain. The results indicate that the upstream and downstream lengths do not affect the Strouhal number. However, the influence on the other parameters has been noticed to be very important. The best indicator for changes in the streamwise length is the rms lift coefficient, that was more sensitive to variations in the numerical domain. According to the results obtained, suggestions are furnished for the choices on the computational domain dimension. It is important to stress that the choice for the values will depend also of mesh size and the power processing for the domains employed in the simulations.

The changes in the height of the computational domain imply in different blockage ratios. These effects were investigated for small and high blockage. For the cases studied the lift and drag forces and Strouhal numbers all rise with blockage ratio.

The flow patterns have been analyzed by means of the streamline and vorticity contours. It has been observed that the vortices are formed more densely for high blockage ratios and consequently this indicates a larger Strouhal number. At high blockage, the streamlines present an oscillatory pattern with small curvature radius.

The Strouhal number has been investigated for different Reynolds numbers with the use of a computational grid chosen according to the recommendations. The results indicate a good agreement between numerical and experimental data.

### ***Acknowledgments***

This study has been developed with financial support provided by FAPESP (proc. 98/12990-3). The authors thank the support of the PROPP/UNESP.

### **5. REFERENCES**

- Davis, R. W. & Moore, E. F., 1982, A numerical study of vortex shedding from rectangles, *J. Fluid Mech.*, vol.116, pp.475-506.
- Fromm, J. E. & Harlow, F. H., 1963, Numerical solution of the problem of vortex street development, *Physics of Fluids*, vol.6, n.7., pp.975-982.
- Leonard, B. P., 1979, A stable and accurate convective modelling procedure based on quadratic upstream interpolation, *Comp. Meth. Appl. Mech. & Engng*, pp.59-98.
- Lindquist, C., 2000, Estudo experimental do escoamento ao redor de cilindros de base quadrada e retangular, Tese de mestrado - UNESP/FEIS.
- Okajima, A., 1982, Strouhal numbers of rectangular cylinders, *J. Fluid Mech.*, vol.123, pp.379-398.
- Patankar, S. V. & Spalding, D. B., 1972, A calculation procedure for heat and mass transfer in three-dimensional parabolic flows, *Journal of Heat and Mass Transfer*, vol.15, pp.1787-1806.
- Sohankar, A., Davidson, L. & Norberg, C., 1995, Numerical simulation of unsteady flow around a square two-dimensional cylinder, *Proceeding 12<sup>th</sup> Australasian Fluid Mechanics Conference*, R. W. Bilger (ed.), pp.517-520.
- Sohankar, A., Davidson, L., & Norberg, C., 1997, Numerical simulation of unsteady low-Reynolds number flow around a rectangular cylinders at incidence, *Journal of Wind Engineering and Industrial Aerodynamics*, vol.69-71, pp.189-201.
- Sohankar, A., Norberg, C., & Davidson, L., 1998, Low-Reynolds flow around a square cylinder at incidence: study of blockage, onset of vortex shedding and outlet boundary condition, *International Journal for Numerical Methods in Fluids*, vol.26, pp.39-56.
- Yu, D. & Kareem, A., 1997, Numerical simulation of flow around rectangular prism, *Journal of Wind Engineering and Industrial Aerodynamics*, vol.67/68, pp.195-208.